

COLUMBIA UNIVERSITY

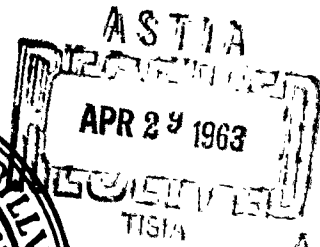
402 680

GUIDED ELECTROMAGNETIC PROPAGATION  
ALONG A NON-GYROTROPIC CIRCULAR PLASMA COLUMN

by

V. L. Granatstein and S. P. Schlesinger

CATALOGED BY ASTIA  
AS AD NO. 402680



DEPARTMENT OF ELECTRICAL ENGINEERING  
SCHOOL OF ENGINEERING  
COLUMBIA UNIVERSITY  
NEW YORK 27, N. Y.

Columbia University  
in the City of New York

A CESIUM PLASMA DIODE

by

B. Pariser and R. A. Gross

Part of the National Science Foundation  
new laboratory equipment development project;  
NSF Grant 17701

January 1963



PLASMA LABORATORY  
SCHOOL OF ENGINEERING AND APPLIED SCIENCE  
NEW YORK 27, N.Y.

AFCRL-63-10

CU-23-62-AF-3879-EE

GUIDED ELECTROMAGNETIC PROPAGATION  
ALONG A NON-GYROTROPIC CIRCULAR PLASMA COLUMN

by

V. L. Granatstein and S. P. Schlesinger

Columbia University  
Department of Electrical Engineering  
New York 27, New York  
Contract No. AF 19(604)-3879  
Project No. 4600

Scientific Report No. 77

October 30, 1962

Prepared for

Electronics Research Directorate  
Air Force Cambridge Research Laboratories  
Office of Aerospace Research  
United States Air Force  
Bedford, Massachusetts

Requests for additional copies by agencies of the Department of Defense, their contractors, and other government agencies should be directed to the

ARMED SERVICES TECHNICAL INFORMATION AGENCY  
ARLINGTON HALL STATION  
ARLINGTON 12, VIRGINIA

Department of Defense contractors must be established for ASTIA services, or have their "need-to-know" certified by the cognizant military agency of their project or contract.

All other persons and organizations should apply to the

U. S. DEPARTMENT OF COMMERCE  
OFFICE OF TECHNICAL SERVICES  
WASHINGTON 25, D. C.

ABSTRACT

Guided electromagnetic modes along a homogeneous circular column of plasma imbedded in free space are examined for the two extreme cases of zero and large axial magnetic field. The plasma is assumed to be cold and collisionless and ion motion is neglected. The assumptions made are approximated by certain laboratory plasmas and hence the results may be of practical importance.

For the zero field case the modes with azimuthal variation are found under certain conditions to exhibit backward wave characteristics and previously published results of a quasi-static analysis are modified. In the case of large magnetic field, the occurrence of unique waveguiding features is discussed.

TABLE OF CONTENTS

ABSTRACT

I.	INTRODUCTION	1
II.	BASIC EQUATIONS	3
	A. Capacitivity Tensor	3
	B. The Fields of a Magneto Plasma	4
	C. Solutions in the Free Space Region	7
III.	THE PLASMA COLUMN IN ZERO MAGNETIC FIELD	9
	A. The Characteristic Equation	9
	B. The Dispersion Curves	16
	C. Comparison with Quasi-Static Analysis	23
IV.	THE PLASMA COLUMN IN LARGE AXIAL MAGNETIC FIELD	25
	A. The Dispersion Curves	25
	B. A Unique Waveguiding Feature	28
V.	CONCLUSIONS	33
	LIST OF REFERENCES	34

## I. INTRODUCTION

This study is concerned with the high frequency modes of guided electromagnetic propagation along a circular plasma column of infinite length and finite radius,  $b$ , as shown in Fig. 1. The plasma density is homogeneous for  $r < b$  and decreases discontinuously to zero at  $r = b$  where a free space region begins. There may also be present a d.c. axial magnetic field,  $B_0$ .

Specifically the cases of  $B_0 = 0$  and  $B_0 \rightarrow \infty$  are investigated in detail, modes with azimuthally varying fields being included in the investigation. Although it has long been recognized that Maxwell's equations in these two extremes of magnetic field are tractable, previous investigation into the mode structure of an unenclosed column has been incomplete.

Trivelpiece and Gould<sup>1</sup> have presented an exact treatment of the azimuthally symmetric mode, and Trivelpiece<sup>2</sup> has presented a quasi-static treatment for the mode of one angular variation for the unenclosed column in zero magnetic field. The existence of backward waves and cutoff was indicated for the azimuthally varying mode, but the usefulness of these conclusions is limited by the nature of the quasi-static assumptions.

Linhart<sup>3</sup> has examined the dispersion curves for the circularly symmetric modes in the limit of large magnetic field.

This paper begins with a tutorial derivation of some basic equations governing high frequency wave propagation in a homogeneous plasma for the general case of arbitrary magnetic field. Subsequent sections apply these equations to the derivation of dispersion curves for the two extreme cases under investigation.

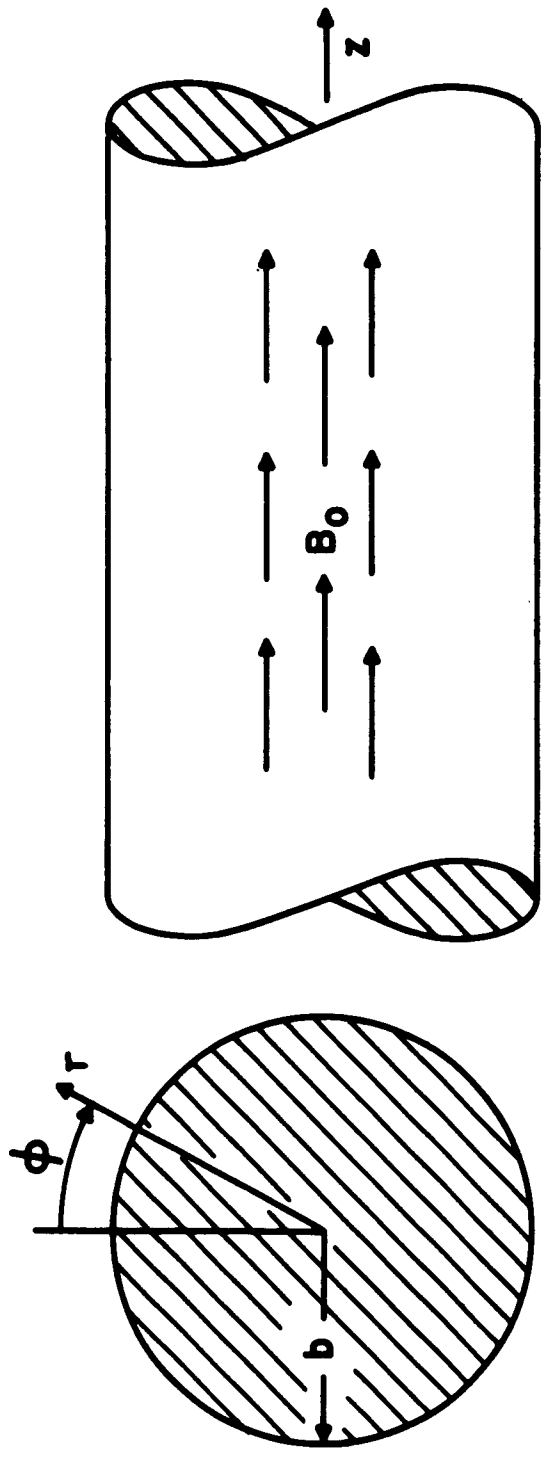


Figure 1 The Open Circular Cylindrical Plasmaguide



II. BASIC EQUATIONS

A. Capacitivity Tensor

A plasma may be represented by a tensor capacitvity whose substitution into Maxwell's equations yields the field defining equations. The use of a tensor of relatively simple form involves the adoption of an idealized plasma model. The plasma is assumed to consist of a cold collisionless electron gas of density,  $n$ , imbedded in a stationary background of neutralizing ions in the presence of an axial magnetic field,  $B_0$ . Then with linearization appropriate to small signals the motion of the electrons is given simply as the response to a Lorentz force

$$m\dot{\underline{v}} = -e[\underline{E} + \underline{v} \times B_0] \quad (1)$$

where  $m$  is the electron mass

$e$  is the magnitude of electron charge

$\underline{v}$  is the electron velocity.

By defining a polarization current density  $\dot{\underline{P}} = ne\underline{v}$  and assuming time dependence as  $e^{j\omega t}$ , the polarization  $\underline{P}$  may be easily determined from (1).

Then, setting  $\underline{D} = \underline{\epsilon} \cdot \underline{E} = \epsilon_0 \underline{E} + \underline{P}$  defines the tensor capacitvity  $\underline{\epsilon}$ .

$$\begin{bmatrix} D_{T1} \\ D_{T2} \\ D_z \end{bmatrix} = \epsilon_0 \begin{bmatrix} 1 - \frac{\omega_p^2}{\omega^2 - \omega_c^2} & -j \frac{\omega_p^2 \omega_c}{\omega(\omega^2 - \omega_c^2)} & 0 \\ j \frac{\omega_p^2 \omega_c}{\omega(\omega^2 - \omega_c^2)} & 1 - \frac{\omega_p^2}{\omega^2 - \omega_c^2} & 0 \\ 0 & 0 & 1 - \frac{\omega_p^2}{\omega^2} \end{bmatrix} \begin{bmatrix} E_{T1} \\ E_{T2} \\ E_z \end{bmatrix}$$

$$= \begin{bmatrix} \epsilon_1 & j\epsilon_2 & 0 \\ -j\epsilon_2 & \epsilon_1 & 0 \\ 0 & 0 & \epsilon_3 \end{bmatrix} \begin{bmatrix} E_{T1} \\ E_{T2} \\ E_z \end{bmatrix} \quad (2)$$

where  $T_1, T_2$  are subscripts denoting arbitrary orthogonal coordinates transverse to the axis

$$\omega_p = \left( \frac{ne^2}{\epsilon_0 m} \right)^{1/2} \text{ is the radian electron plasma frequency.}$$

$$\omega_c = \frac{eB_0}{m} \text{ is the radian electron cyclotron frequency.}$$

### B. The Fields of a Magneto Plasma

Consider Maxwell's equations in general orthogonal cylindrical coordinates with line element  $ds^2 = h_1^2 dq_1^2 + h_2^2 dq_2^2 + dz^2$  in a homogeneous medium whose capacitivity has the form of (2) and whose permeability equals the free space value,  $\mu_0$ . The curl equations may be written

$$(\nabla_T - j\beta \hat{\lambda}_z) \times (\underline{E}_T + E_z \hat{\lambda}_z) = -j\omega \mu_0 (\underline{H}_T + H_z \hat{\lambda}_z) \quad (3)$$

$$(\nabla_T - j\beta \hat{\lambda}_z) \times (\underline{H}_T + H_z \hat{\lambda}_z) = j\omega (\epsilon_T \cdot \underline{E}_T + \epsilon_z E_z \hat{\lambda}_z) \quad (4)$$

where  $T$  denotes the transverse part and axial variation as  $e^{-j\beta z}$  is assumed.

Equating the transverse parts in (3) and (4) yields the dependency equations which express the transverse field components in terms of the axial components

$$\underline{E}_T = -j\omega \mu_0 \underline{A}^{-1} \cdot (\nabla_T \times \hat{\lambda}_z H_z) - j\beta \underline{A}^{-1} \cdot \nabla_T E_z \quad (5)$$

$$\underline{H}_T = \frac{j}{\omega \mu_0} \nabla_T \times \hat{\lambda}_z E_z + \frac{\beta}{\omega \mu_0} \hat{\lambda}_z \times \underline{E}_T \quad (6)$$

$$\text{where } \underline{A} = [\omega^2 \mu_0 \epsilon_T - \beta^2 \underline{I}] \quad (7)$$

It remains to find wave type equations governing the axial field components. We proceed as is usual by taking the curl of (3) and substituting from (4) which gives

$$\begin{aligned} \nabla \times \nabla \times \underline{E} &= -(\nabla_T^2 - \beta^2) (\underline{E}_T + E_z \hat{\lambda}_z) + (\nabla_T - j\beta \hat{\lambda}_z) (\nabla_T - j\beta \hat{\lambda}_z) \cdot (\underline{E}_T + \hat{\lambda}_z E_z) \\ &= \omega^2 \mu_0 (\underline{\epsilon}_T \cdot \underline{E}_T + \epsilon_3 E_z \hat{\lambda}_z) \end{aligned} \quad (8)$$

Equating the axial components of (8) gives

$$\nabla_T^2 E_z + \omega^2 \mu_0 \epsilon_3 E_z = j\beta \nabla_T \cdot \underline{E}_T \quad (9)$$

In a similar manner by taking the curl of (4) one may show that

$$\nabla_T^2 H_z - \beta^2 H_z = -j\omega (\nabla_T \times \underline{\epsilon}_T \cdot \underline{E}_T) \cdot \hat{\lambda}_z \quad (10)$$

The expressions on the right of (9) and (10) must now be expressed in terms of the axial components. To get an expression for  $\nabla \cdot \underline{E}_T$  we consider  $\nabla_T \cdot (\underline{\epsilon} \cdot \underline{E}_T)$  since this is known to equal  $j\beta \epsilon_3 E_z$  from  $\nabla \cdot \underline{D} = 0$ . In the notation of general curvilinear coordinates

$$\begin{aligned} \nabla_T \cdot (\underline{\epsilon}_T \cdot \underline{E}_T) &= \frac{1}{h_1 h_2} \left[ \frac{\partial}{\partial q_1} (h_1 \epsilon_1 E_1 + j h_2 \epsilon_2 E_2) + \frac{\partial}{\partial q_2} (-j h_1 \epsilon_2 E_1 + h_1 \epsilon_1 E_2) \right] \\ &= \epsilon_1 \left[ \frac{1}{h_1 h_2} \left\{ \frac{\partial}{\partial q_1} (h_2 E_1) + \frac{\partial}{\partial q_2} (h_1 E_2) \right\} \right] + j \epsilon_2 \left[ \frac{1}{h_1 h_2} \left\{ \frac{\partial}{\partial q_1} (h_2 E_2) - \frac{\partial}{\partial q_2} (h_1 E_1) \right\} \right] \\ &= \epsilon_1 \nabla_T \cdot \underline{E}_T + \omega \mu_0 \epsilon_2 H_z \end{aligned}$$

so that

$$\nabla_T \cdot \underline{E}_T = j\beta \frac{\epsilon_3}{\epsilon_1} E_z - \omega \mu_0 \frac{\epsilon_2}{\epsilon_1} H_z \quad (11)$$

In a similar manner we may evaluate

$$(\nabla_T \times \underline{\epsilon}_T \cdot \underline{E}_T) \cdot \hat{z} = \frac{\beta \epsilon_2 \epsilon_3}{\epsilon_1} E_z + j\omega\mu_0 \left( \frac{\epsilon_2^2}{\epsilon_1} - \epsilon_1 \right) H_z \quad (12)$$

Then substituting (11) into (9) and (12) into (10) produces the desired wave type equations

$$\nabla_T^2 E_z + \left( \omega^2 \mu_0 \epsilon_3 - \frac{\epsilon_3}{\epsilon_1} \beta^2 \right) E_z = j\beta\omega\mu_0 \frac{\epsilon_2}{\epsilon_1} H_z \quad (13)$$

$$\nabla_T^2 H_z + \left( \omega^2 \mu_0 \frac{\epsilon_1^2 - \epsilon_2^2}{\epsilon_1} - \beta^2 \right) H_z = -j\beta\omega \frac{\epsilon_2 \epsilon_3}{\epsilon_1} E_z \quad (14)$$

In circular cylindrical coordinates with azimuthal variation as  $e^{-jn\phi}$  the dependency equations (5) and (6) become

$$\begin{bmatrix} \omega^2 \mu_0 \epsilon_1 - \beta^2 & j\omega^2 \mu_0 \epsilon_2 \\ -j\omega^2 \mu_0 \epsilon_2 & \omega^2 \mu_0 \epsilon_1 - \beta^2 \end{bmatrix} \begin{bmatrix} E_r \\ E_\phi \end{bmatrix} = \begin{bmatrix} -j\beta \frac{\partial}{\partial r} & \frac{-n\omega\mu_0}{r} \\ \frac{-n\beta}{r} & j\omega\mu_0 \frac{\partial}{\partial r} \end{bmatrix} \begin{bmatrix} E_z \\ H_z \end{bmatrix} \quad (15)$$

$$\begin{bmatrix} H_r \\ H_\phi \end{bmatrix} = \begin{bmatrix} 0 & \frac{-\beta}{\omega\mu_0} & \frac{n}{\omega\mu_0 r} \\ \frac{\beta}{\omega\mu_0} & 0 & -j \frac{1}{\omega\mu_0} \frac{\partial}{\partial r} \end{bmatrix} \begin{bmatrix} E_r \\ E_\phi \\ E_z \end{bmatrix} \quad (16)$$

and the coupled wave equations in the axial components become

$$\frac{1}{r} \frac{\partial}{\partial r} \left( r \frac{\partial E_z}{\partial r} \right) + \left( \frac{\omega^2}{c^2} \frac{\epsilon_3}{\epsilon_0} - \frac{\epsilon_3}{\epsilon_1} \beta^2 - \frac{n^2}{r^2} \right) E_z = j\beta\omega\mu_0 \frac{\epsilon_2}{\epsilon_1} H_z \quad (17)$$

$$\frac{1}{r} \frac{\partial}{\partial r} \left( r \frac{\partial H_z}{\partial r} \right) + \left( \frac{\omega^2}{c^2} \frac{\epsilon_1^2 - \epsilon_2^2}{\epsilon_1 \epsilon_0} - \beta^2 - \frac{n^2}{r^2} \right) H_z = -j\beta\omega \frac{\epsilon_2 \epsilon_1}{\epsilon_3} E_z \quad (18)$$

Equations equivalent to (15), (16), (17) and (18) have previously appeared in the literature<sup>4,5</sup>. They are in general applicable to any medium with tensor capacitivity of the form shown in (2) and by a scalar permeability. In particular, we will apply them to a plasma in two limits of magnetic field where degenerate forms of the capacitivity tensor hold and the wave equations become uncoupled.

These field equations are also of course applicable to the very degenerate case of free space, and we next proceed to use them in finding the fields of the free space region surrounding the plasma column.

### C. Solutions in the Free Space Region

In free space the use of equations (15), (16), (17) and (18) entails setting  $\epsilon_2 = 0$  and  $\epsilon_1 = \epsilon_3 = \epsilon_0$ . The wave equations uncouple and reduce to Bessel equations with eigennumber  $\frac{\omega^2}{c^2} - \beta^2$ . The appropriate solutions for bound modes are hyperbolic Bessel functions  $K_n\left(\frac{qr}{b}\right)$  where

$$q^2 = \beta^2 b^2 - \frac{\omega^2}{c^2} b^2 \quad (19)$$

$q$  is real indicating that  $\beta > \frac{\omega}{c}$ .

The axial field components are then given by

$$E_{z0} = A K_n\left(\frac{qr}{b}\right) e^{j(\omega t - \beta z - n\phi)} \quad H_{z0} = B K_n\left(\frac{qr}{b}\right) e^{j(\omega t - \beta z - n\phi)} \quad (20)$$

where  $A$  and  $B$  are constants to be determined by conditions at the interface  $r = b$ , and by the strength of excitation.

The transverse fields may be found from (15) and (16), the azimuthal components being

$$H_{\phi 0} = \left[ A \frac{j\omega \epsilon_0 b^2}{q^2} \frac{\partial}{\partial r} K_n\left(\frac{qr}{b}\right) + B \frac{n\beta b^2}{q^2 r} K_n\left(\frac{qr}{b}\right) \right] e^{j(\omega t - \beta z - n\phi)} \quad (21)$$

$$E_{\phi 0} = \left[ A \frac{n\beta b^2}{q^2 r} K_n\left(\frac{qr}{b}\right) - B \frac{j b^2 \omega \mu_0}{q^2} \frac{\partial}{\partial r} K_n\left(\frac{qr}{b}\right) \right] e^{j(\omega t - \beta z - n\phi)} \quad (22)$$

In the next section we obtain the plasma fields and the associated dispersion relationship for a plasma column in zero magnetic field.

### III. THE PLASMA COLUMN IN ZERO MAGNETIC FIELD

As mentioned in the introduction, the case of no azimuthal variation ( $n = 0$ ) has been treated previously<sup>1,2</sup>, and therefore this investigation is confined to the higher order modes ( $n \geq 1$ ).

#### A. The Characteristic Equation

##### (a) Derivation

With  $B_0 = 0$  the capacitivity tensor of equation (2) degenerates into the scalar  $\epsilon_0(1 - \frac{\omega_p^2}{\omega^2})$ , and the wave equations, (17) and (18), reduce to Bessel equations with eigennumbers  $\frac{\omega^2}{c^2}(1 - \frac{\omega_p^2}{\omega^2}) - \beta^2$ . The plasma region solutions are accordingly

$$E_{zi} = CI_n\left(\frac{pr}{b}\right) e^{j(\omega t - \beta z - n\phi)} \quad H_{zi} = DI_n\left(\frac{pr}{b}\right) e^{j(\omega t - \beta z - n\phi)} \quad (23)$$

$$p^2 = \beta^2 b^2 - \frac{\omega^2 b^2}{c^2} + \frac{\omega_p^2 b^2}{c^2} = q^2 + \frac{\omega_p^2 b^2}{c^2} \quad (24)$$

Note that the factor  $\frac{\omega_p^2 b^2}{c^2}$  is always positive so that the radial eigennumber in the plasma region,  $p$ , is always greater than that in the free space region,  $q$ . Equation (24) is a hyperbola on the  $p, q$  plane which intercepts the  $q = 0$  axis at  $p = \frac{\omega_p b}{c}$ .

Transverse field components may be determined from equations (15) and (16); the azimuthal components are

$$E_{\phi i} = \left[ C \frac{n\beta b^2}{p^2 r} I_n\left(\frac{pr}{b}\right) - D \frac{j\omega\mu_0 b^2}{p^2} \frac{\partial}{\partial r} I_n\left(\frac{pr}{b}\right) \right] e^{j(\omega t - \beta z - n\phi)} \quad (25)$$

$$H_{\phi i} = \left[ C \frac{j}{\omega\mu_0} \left( \frac{\beta^2 b^2}{p^2} - 1 \right) \frac{\partial}{\partial r} I_n\left(\frac{pr}{b}\right) + D \frac{\beta n b^2}{r p^2} I_n\left(\frac{pr}{b}\right) \right] e^{j(\omega t - \beta z - n\phi)} \quad (26)$$

Imposing the condition that the tangential ( $\phi$  and  $z$ ) field components be matched at the boundary  $r = b$  gives a set of four homogeneous equations in A, B, C and D. For nontrivial solutions the determinant of the coefficient matrix must be set equal to zero, which results as usual in the characteristic equation. It proves convenient to formulate the characteristic equation in terms of the following functions,

$$K_n^+(X) = \frac{K_{n+1}(X)}{XK_n(X)}, \quad K_n^-(X) = \frac{K_{n-1}(X)}{XK_n(X)}, \quad I_n^+(X) = \frac{I_{n+1}(X)}{XI_n(X)}, \quad I_n^-(X) = \frac{I_{n-1}(X)}{XI_n(X)} \quad (27)$$

The characteristic equation is then

$$\begin{aligned} [I_n^+(p) + K_n^+(q)] \left[ \left(1 - \frac{\omega_p^2}{\omega^2}\right) I_n^-(p) + K_n^-(q) \right] + [I_n^-(p) + K_n^-(q)] \\ \left[ \left(1 - \frac{\omega_p^2}{\omega^2}\right) I_n^+(p) + K_n^+(q) \right] = 0 \end{aligned} \quad (28)$$

The higher order modes ( $n \geq 1$ ) governed by this equation are hybrid possessing axial components of both  $\underline{E}$  and  $\underline{H}$ . The existence of TE or TM modes would imply  $n(p^2 - q^2) = 0$  which contradicts (24).

The hyperbolic Bessel functions of first and second kind which appear in equation (28) are monotonic, indicating the existence of a single mode for each value of  $n$ .

(b) Non-Existence of Solutions for  $\omega > \frac{\omega_p}{\sqrt{2}}$

It may be shown that no solutions exist for (28) when  $\omega > \frac{\omega_p}{\sqrt{2}}$ . This implies that for the existence of guided waves there is a maximum frequency limit or equivalently the constraint that the capacitivity must be negative and greater in magnitude than  $\epsilon_0$ .

The characteristic equation (28) may be written in the form



$$\frac{\omega^2}{\omega^2} = 1 + \frac{2 K_n^+(q) K_n^-(q) + K_n^+(q) I_n^-(p) + K_n^-(q) I_n^+(p)}{2 I_n^-(p) I_n^+(p) + K_n^+(q) I_n^-(p) + K_n^-(q) I_n^+(p)} \quad (29)$$

Demonstration of the fact that  $\omega < \frac{\omega_p}{\sqrt{2}}$  is thus equivalent to showing that  $K_n^+(q) K_n^-(q) > I_n^-(p) I_n^+(p)$  which may be expanded as

$$\frac{p^2}{q^2} \frac{K_{n+1}(q) K_{n-1}(q)}{K_n^2(q)} > \frac{I_{n-1}(p) I_{n+1}(p)}{I_n^2(p)} \quad (30)$$

Note the following integral expressions<sup>6</sup> for the products of hyperbolic Bessel functions.

$$K_\mu(q) K_\nu(q) = 2 \int_0^\infty K_{\mu+\nu}(2q \cosh t) \cosh(\mu-\nu)t \, dt \quad (31)$$

$$I_\mu(p) I_\nu(p) = \frac{2}{\pi} \int_0^{\pi/2} I_{\mu+\nu}(2p \cos \theta) \cos(\mu-\nu)\theta \, d\theta \quad (32)$$

From (31),

$$K_{n+1}(q) K_{n-1}(q) = 2 \int_0^\infty K_{2n}(2q \cosh t) \cosh 2t \, dt \quad (33)$$

and 
$$K_n^2(q) = 2 \int_0^\infty K_{2n}(2q \cosh t) \, dt \quad (34)$$

Now  $\cosh 2t \geq 1$ , and  $q$  is real so that the integrands in (33) and (34) are always positive. Thus we see

$$K_{n-1}(q) K_{n-1}(q) \geq K_n^2(q) \quad (35)$$

In a similar manner using (32), it may be shown that

$$I_n^2(p) \geq I_{n+1}(p) I_{n-1}(p) \quad (36)$$

Then (35) and (36) together with the fact that  $p > q$  establish the required inequality (30).

(c) Cutoff and Resonance

The characteristic equation (28) is represented by the solid lines in Fig. 2 for  $n = 1$  and in Fig. 3 for  $n = 2$  for various values of the parameter  $\frac{\omega_p^2}{\omega^2}$ . The features of the curves for  $n = 2$  may be taken as representative for modes of larger  $n$ .

Note that the curves for  $n = 1$  begin at the origin of the  $p, q$  plane whereas for  $n = 2$  the curves intersect the  $q = 0$  axis at some non-zero value of  $p$ . Also, both sets of curves intersect the line  $p = q$  for small values of  $\frac{\omega_p^2}{\omega^2}$ . These features are of physical significance and it is of value to trace their occurrence mathematically.

The  $q = 0$  axis represents a cutoff for bound modes; from (19) it may be seen that at  $q = 0$ ,  $\beta = \frac{\omega}{c}$  which is the transition point between slow and fast waves. The line  $q = p$  is a resonance since from (24) it implies  $\beta \rightarrow \infty$ .

At cutoff ( $q = 0$ ), note the following limits of the functions of  $q$  appearing in (28)

$$\lim_{q \rightarrow 0} K_n^+(q) = \frac{2n}{q^2}, \quad n \geq 1 \quad (37)$$

$$\lim_{q \rightarrow 0} K_n^-(q) = -\ln q, \quad n = 1 \quad (38)$$

$$\lim_{q \rightarrow 0} K_n^-(q) = \frac{1}{2(n-1)}, \quad n > 1 \quad (39)$$

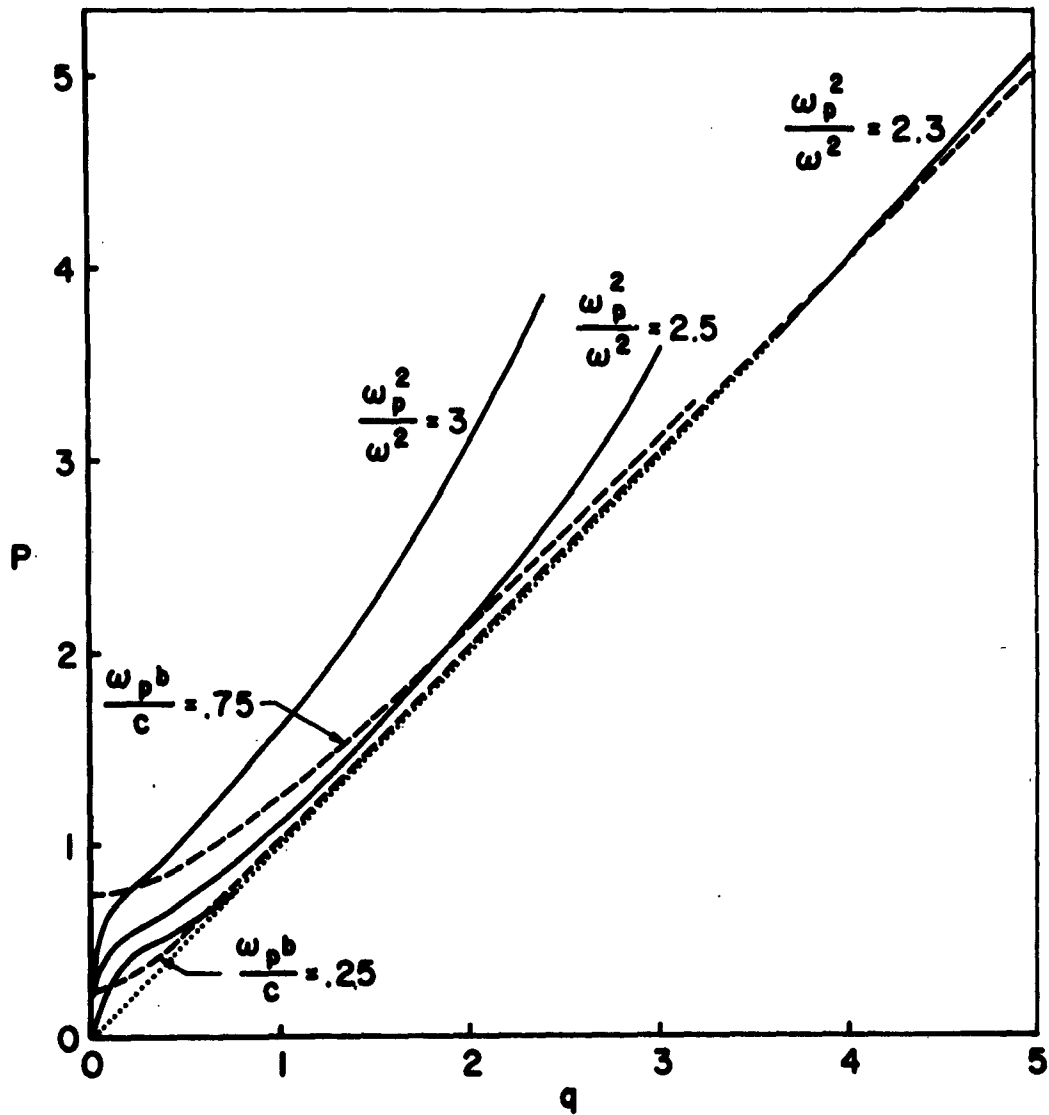


Figure 2 Characteristic Equation for the Plasma Column in Zero Magnetic Field,  $n = 1$

— equation (28)  
- - - equation (24)  
..... (  $P = q$  )

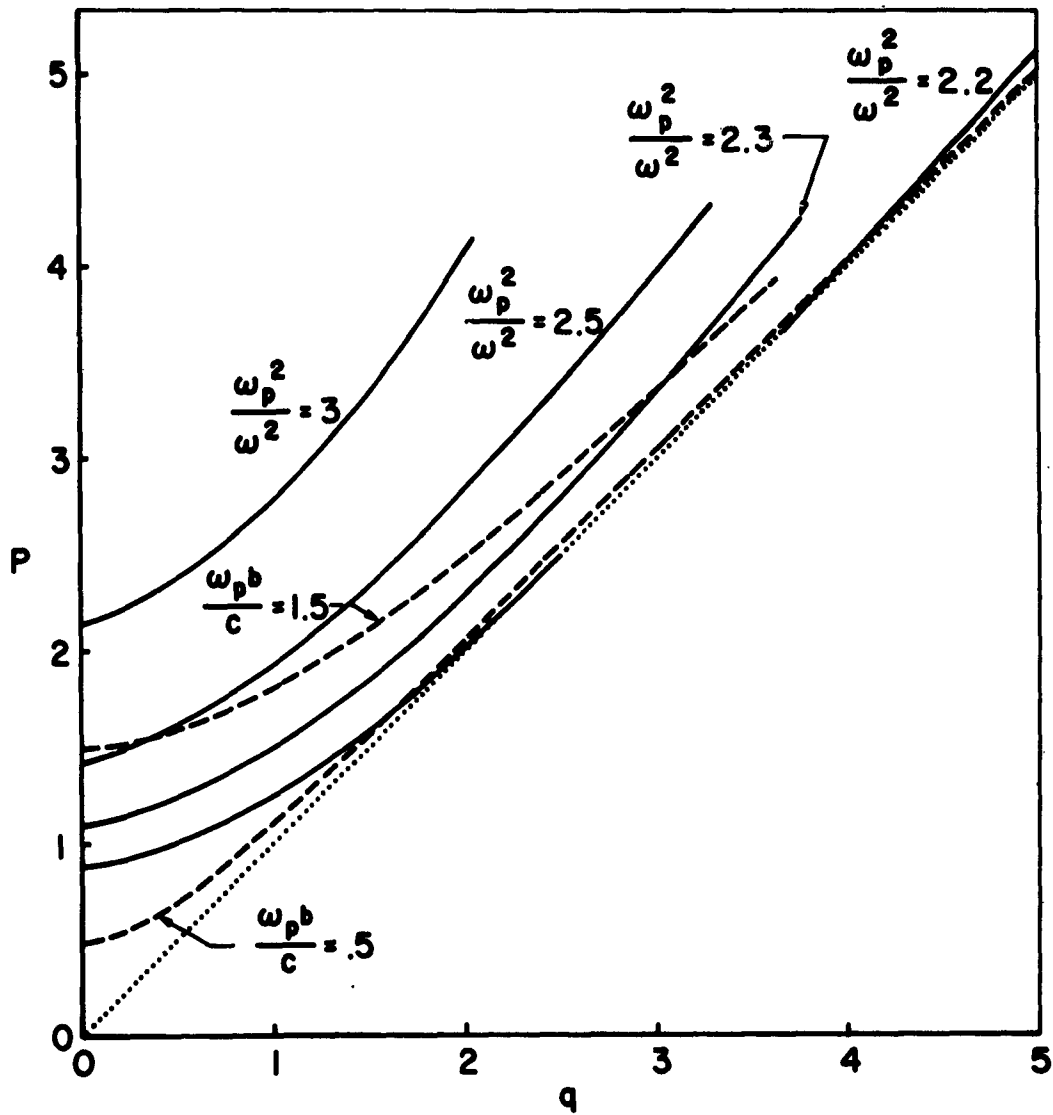


Figure 3 Characteristic Equation for the Plasma Column in Zero Magnetic Field,  $n = 2$

- equation (28)
- - - - - equation (24)
- ..... (  $p = q$  )

Because of the distinct cases in (38) and (39) the  $n = 1$  mode must be treated separately from  $n > 1$ .

For the mode of one angular variation, the characteristic equation in the cutoff limit becomes

$$\lim_{q \rightarrow 0} \left\{ \frac{2n}{q^2} \left[ \left( 2 - \frac{\omega_p^2}{\omega^2} \right) I_n^-(p) - 2 \ln q \right] \right\} = 0 \quad (40)$$

where the finite nature of  $I_n^+(p)$  has been considered. Equation (40) can be satisfied for nonzero  $\omega$  only when  $I_n^-(p) \rightarrow \infty$  which implies  $p = 0$ . This result will be seen to lead to a zero cutoff frequency for the  $n = 1$  mode.

For the modes with  $n \geq 1$ , the characteristic equation at cutoff for nonzero  $\omega$  becomes

$$\lim_{q \rightarrow 0} \left\{ \frac{2n}{q^2} \left[ \left( 2 - \frac{\omega_p^2}{\omega^2} \right) I_n^-(p) + \frac{1}{n-1} \right] \right\} = 0 \quad (41)$$

This can be satisfied only when

$$I_n^-(p) = \frac{1}{\left( \frac{\omega_p^2}{\omega^2} - 2 \right) (n-1)} \quad (42)$$

The value of  $p$  defined by (42) is the intercept on the  $q = 0$  axis which starts at  $p = 0$  for the marginal case  $\frac{\omega_p^2}{\omega^2} = 2$  and rises to higher values of  $p$  with decreasing  $\omega$ . The nonzero value of the intercept will be seen to imply a nonzero cutoff frequency for modes with  $n > 1$ .

---

Next consider the resonance limit  $q = p$ . The characteristic equation (28) becomes

$$\begin{aligned} & (I_{n+1} K_n + K_{n+1} I_n) \left( \left[ 1 - \frac{\omega_p^2}{\omega^2} \right] I_{n-1} K_n + K_{n-1} I_n \right) \\ & + (I_{n-1} K_n + K_{n-1} I_n) \left( \left[ 1 - \frac{\omega_p^2}{\omega^2} \right] I_{n+1} K_n + K_{n+1} I_n \right) = 0 \end{aligned} \quad (43)$$

where the argument of both the I and K functions is  $p$ .

The identity

$$I_{n+1}(p) K_n(p) + K_{n+1}(p) I_n(p) = \frac{1}{p} \quad (44)$$

may be used to reduce (43) to the form

$$2 \frac{\omega^2}{\omega_p^2} = p [I_{n-1}(p) + I_{n+1}(p)] K_n(p) \quad (45)$$

This relationship is sketched in figure 4.

It will be noted that for small  $\frac{\omega}{\omega_p}$  equation (45) does not have a solution. However, for values of  $\omega$  approaching  $\frac{\omega_p}{\sqrt{2}}$  there are two values of  $p$  which satisfy (45) for a given  $\frac{\omega}{\omega_p}$ . It will subsequently be shown that these solutions indicate the presence of backward waves.

### B. The Dispersion Curves

Substituting for  $p$  and  $q$  from (24) and (19) into the characteristic equation (28) results in a dispersion relationship between  $\frac{\omega b}{c}$  and  $\beta b$  with  $\frac{\omega_p b}{c}$  as a parameter.

$$\begin{aligned} & \left[ I_n^+(p) + K_n^+(q) \right] \left[ \left\{ 1 - \left( \frac{\omega_p b}{c} \right)^2 \left( \frac{\omega b}{c} \right)^{-2} \right\} I_n^-(p) + K_n^-(q) \right] \\ & + \left[ I_n^-(p) + K_n^-(q) \right] \left[ \left\{ 1 - \left( \frac{\omega_p b}{c} \right)^2 \left( \frac{\omega b}{c} \right)^{-2} \right\} I_n^+(p) + K_n^+(q) \right] = 0 \\ & q = \left[ (\beta b)^2 - \left( \frac{\omega b}{c} \right)^2 \right]^{1/2} \quad p = \left[ (\beta b)^2 - \left( \frac{\omega b}{c} \right)^2 + \left( \frac{\omega_p b}{c} \right)^2 \right]^{1/2} \end{aligned} \quad (46)$$

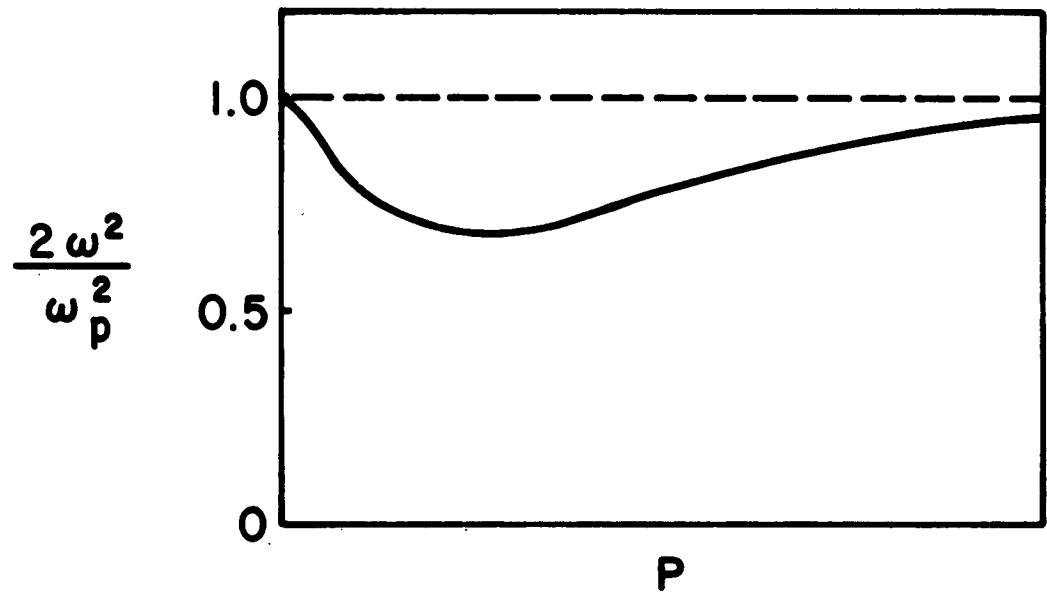


Figure 4 Characteristic Equation Resonance Condition Equation (45)

Points satisfying this equation may be obtained by finding the intersection of a hyperbola

$$p^2 - q^2 = \frac{\omega_p^2 b^2}{c^2} \quad (24)$$

with plots of the characteristic equation for various values of  $(\frac{\omega_p}{\omega})^2$ .

A point of intersection gives  $q$ ,  $p$ ,  $\frac{\omega_p}{\omega}$ , and  $\frac{\omega_p b}{c}$  which yields

$$\frac{\omega b}{c} = \left(\frac{\omega_p b}{c}\right)\left(\frac{\omega}{\omega_p}\right) \text{ and } \beta b = \left(q^2 + \frac{\omega_p^2 b^2}{c^2}\right)^{1/2}.$$

From the hyperbolas for  $\frac{\omega_p b}{c} = .25$  and  $\frac{\omega_p b}{c} = .75$  plotted as dashed lines in figure 2, it may be seen that the dispersion curves for the mode of one angular variation ( $n = 1$ ) passes through the origin,  $\beta b = \frac{\omega b}{c} = 0$ , and asymptotically approaches  $\frac{\omega b}{c} = \frac{1}{\sqrt{2}} \frac{\omega_p b}{c}$  as  $\beta \rightarrow \infty$ . For small values of  $\frac{\omega_p b}{c}$  the dispersion curves will be triple valued in  $\beta$  for a single value of  $\omega$  as indicated by the triple intersection of the hyperbola for  $\frac{\omega_p b}{c} = .25$  with the characteristic equation curve for  $\frac{\omega_p^2}{\omega^2} = 2.3$ ; this implies the existence of a region of negative slope or backward wave propagation.

Hyperbolas for  $\frac{\omega_p b}{c} = .5$  and  $\frac{\omega_p b}{c} = 1.5$  are represented by dashed lines in Fig. 3. The nature of their intersection with the plots of the characteristic equation for  $n = 2$  show that for  $n > 1$  the dispersion curves will begin on the line  $\frac{\omega b}{c} = \beta b$  at some point other than the origin.

This cutoff frequency,  $\omega_{\text{cutoff}}$  is determined from (42) as

$$\omega_{\text{cutoff}} = \omega_p \left( \frac{(n-1) I_n^{-1}\left(\frac{\omega_p b}{c}\right)}{2(n-1) I_n^{-1}\left(\frac{\omega_p b}{c}\right) + 1} \right)^{1/2} \quad (47)$$

The dispersion curves asymptotically approach  $\frac{\omega b}{c} = \frac{1}{\sqrt{2}} \frac{\omega_p b}{c}$ . For small values of  $\frac{\omega_p b}{c}$ , the dispersion curves will be double valued in  $\beta$  again implying the existence of backward wave propagation.



Dispersion curves for  $n = 0$  are reproduced from previously published data<sup>1</sup> in Fig. 5 for purposes of comparison. Dispersion curves for  $n = 1$  are plotted in Fig. 6 and for  $n = 2$  in Fig. 7 for revealing values of the parameter  $\frac{\omega_{pb}}{c}$ . As indicated above, an important difference between the curves for the  $n = 0$  mode and the modes of higher order is the appearance of backward waves in the azimuthally varying modes. The portions of the curves exhibiting this behaviour are enlarged in the lower right corners of Fig. 6 and 7. The phenomena of backward waves must be associated with either the properties of the plasma as a negative dispersive permittivity or with the hybrid nature of the higher order modes or both.<sup>7</sup>

The disappearance of the backward wave characteristics for large values of  $\frac{\omega_{pb}}{c}$  should be noted. Increasing this parameter increases  $p$  relative to  $q$  [see (24)] and this has the effect of decreasing field penetration into the body of the plasma and of concentrating power flow in the free space region as may be seen from consideration of the nature of the hyperbolic Bessel functions.

All three sets of dispersion curves, Fig. 5, 6 and 7, show resonance at  $\omega = \frac{\omega_p}{\sqrt{2}}$ , i.e.,  $\beta$  increases without limit as this frequency is approached. Increasing  $\beta$  implies increasing  $p$  and  $q$  and consequently increasing confinement of field energy to the region of the interface. Furthermore, group velocity  $\partial\omega/\partial\beta$  rapidly approaches zero at the resonance so that energy does not propagate.

As  $\beta$  increases, the phase velocity,  $\omega/\beta$ , of course decreases, and when its value approaches the electron thermal velocity, the assumption of negligible thermal pressure made in section II becomes untenable. An

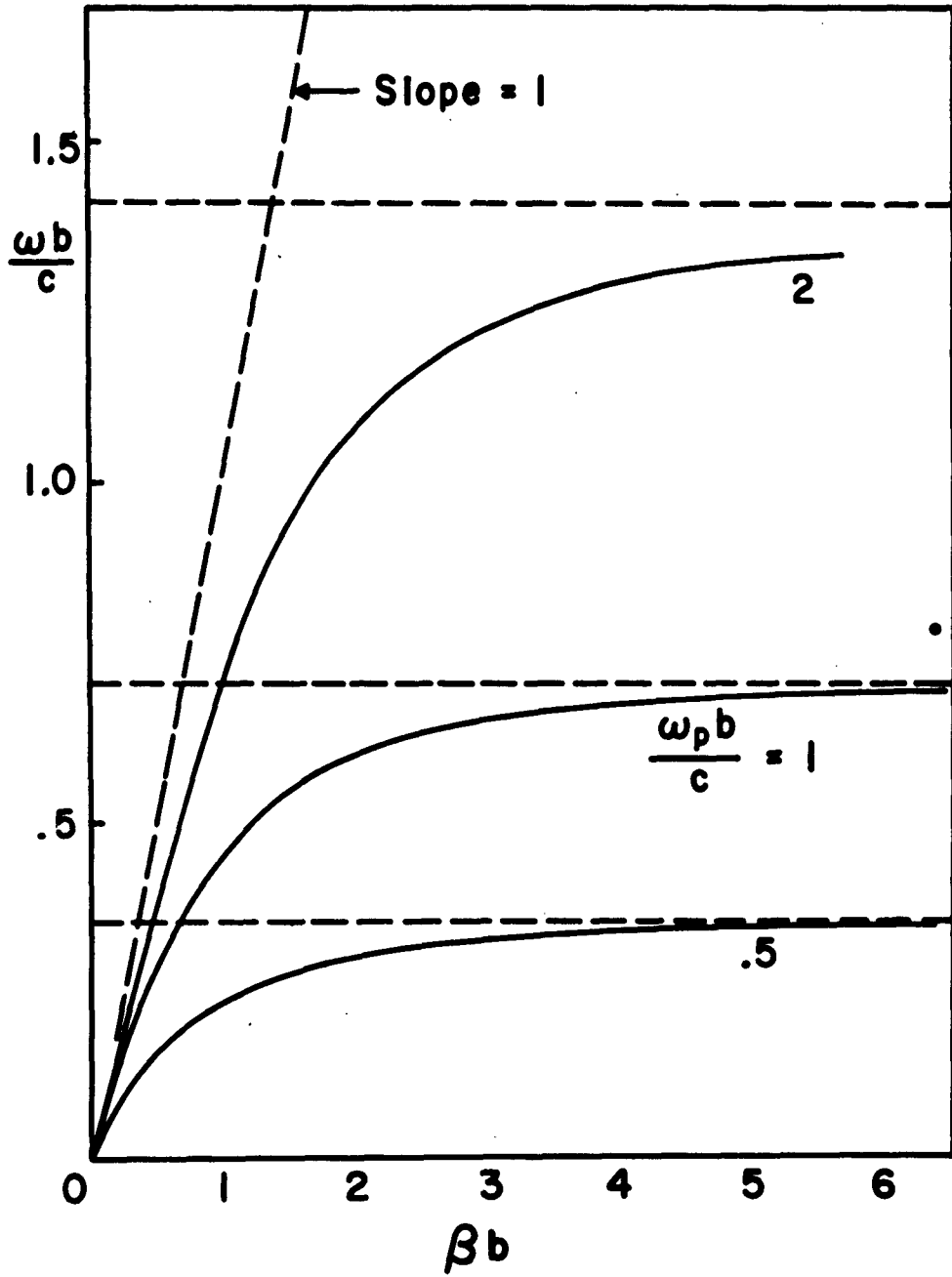


Figure 5 Dispersion Curves for Plasma Column with Zero Magnetic Field,  $n = 0$

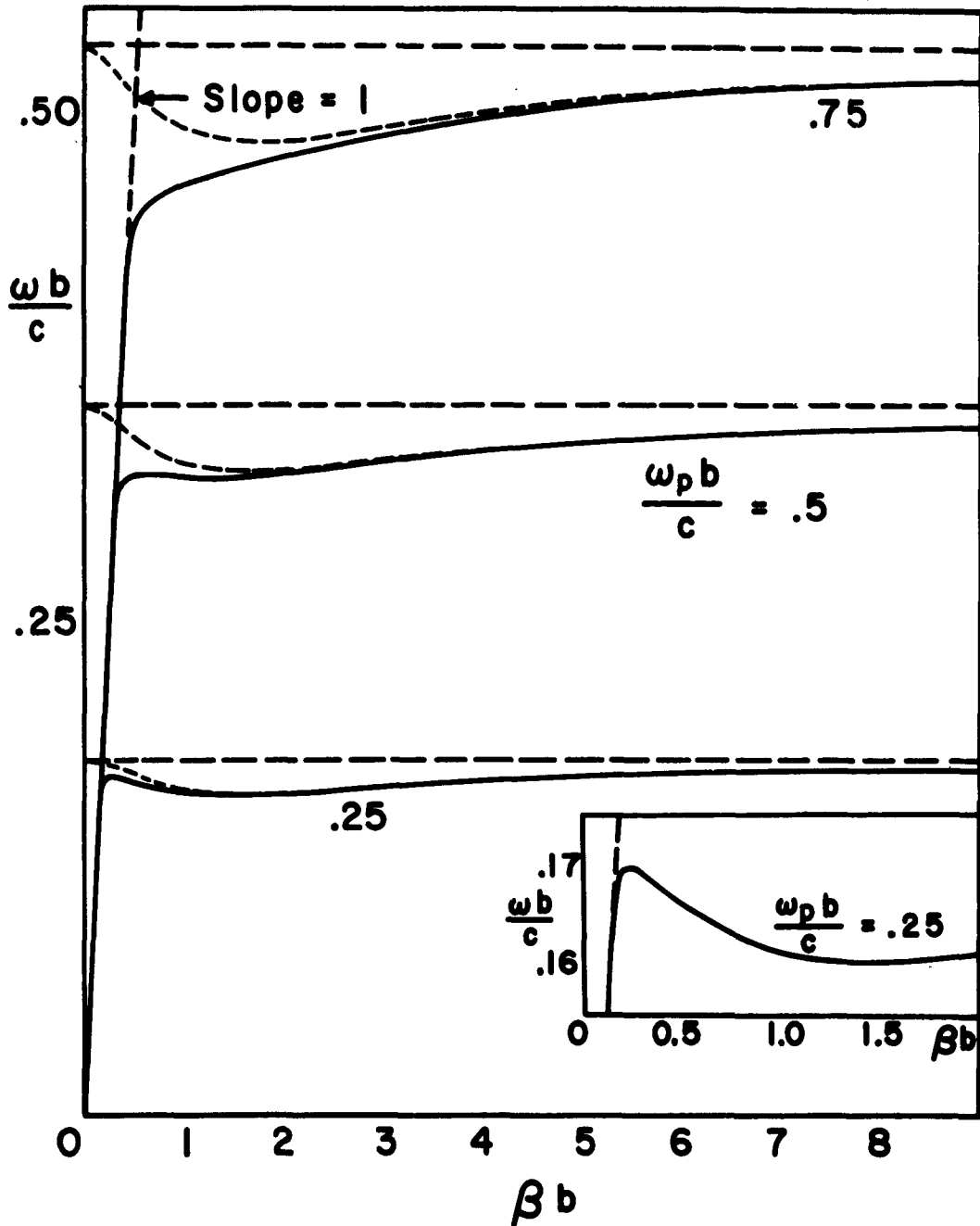


Figure 6 Dispersion Curves for Plasma Column with Zero Magnetic Field,  $n = 1$

———— Rigorous Analysis  
----- Quasi-Static Analysis

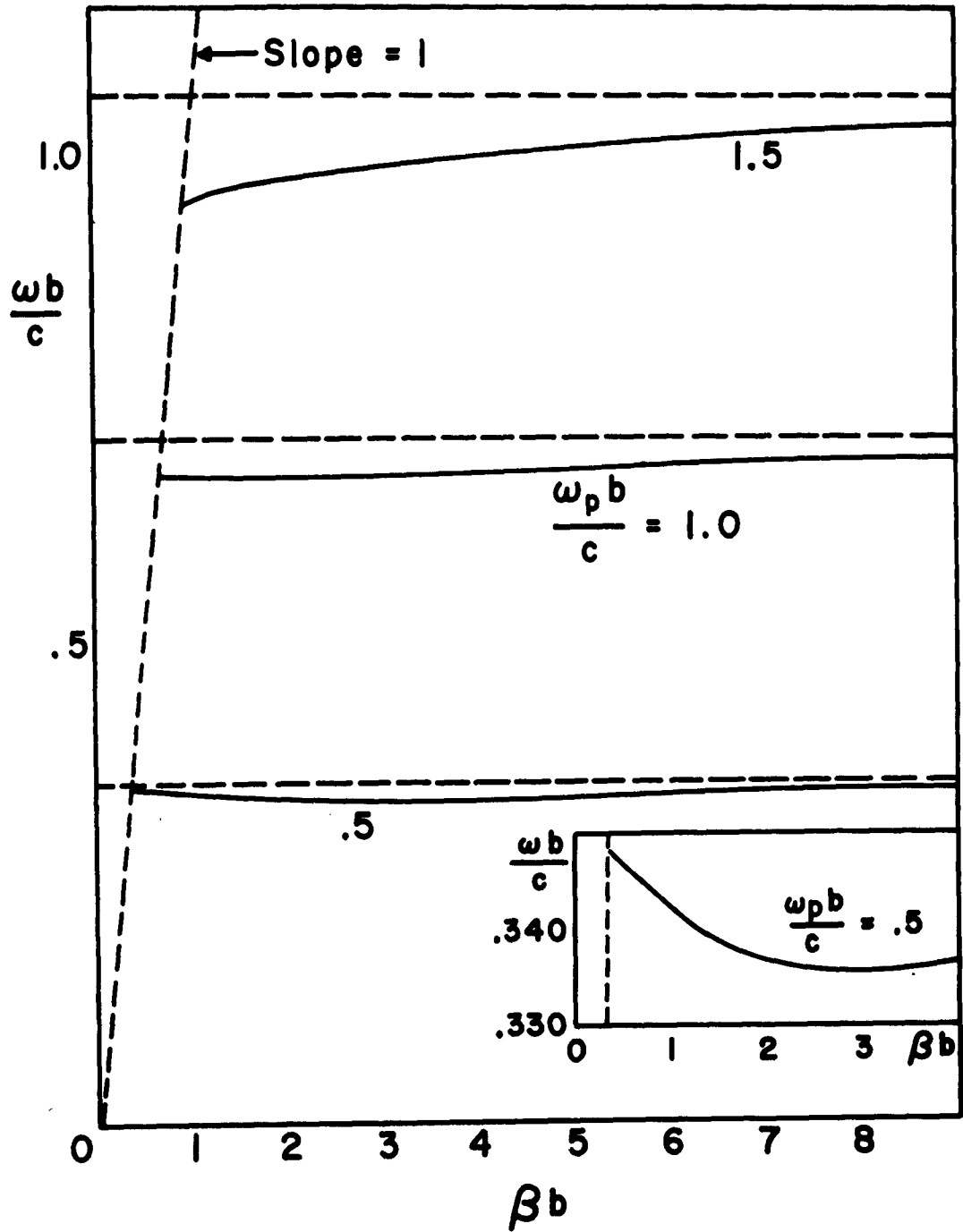


Figure 7 Dispersion Curves for Plasma Column with Zero Magnetic Field,  $n = 2$

analysis that includes the effect of thermal pressure would indicate that as phase velocity approaches electron thermal velocity, damping set in<sup>8,9</sup>, the field energy being converted to electron kinetic energy.

### C. Comparison with Quasi-Static Analysis

It is of interest to compare the modal properties presented above with the predictions of approximate analysis using the quasi-static assumption as carried out by Trivelpiece<sup>2</sup> for the  $n = 1$  mode.

The basic quasi-static assumption is  $\underline{E} = -\nabla V$ ,  $V$  being a scalar potential. For the unmagnetized plasma column this assumption implies not only that  $\beta^2 \gg \frac{\omega^2}{c^2}$  as with non-dispersive media but also that  $\beta^2 \gg \frac{\omega_p^2}{c^2}$ .

The quasi-static assumption leads to the following dispersion equation

$$\frac{\omega_p^2}{\omega^2} - 1 = \frac{K_n^-(\beta b) + K_n^+(\beta b)}{I_n^-(\beta b) + I_n^+(\beta b)} \quad (48)$$

Equation (48) for the  $n = 1$  mode is represented by the dashed lines in Fig. 6. They have intercepts with the  $\beta = 0$  axis at  $\omega = \frac{\omega_p}{\sqrt{2}}$  and corresponding nonzero intercepts with the line  $\beta = \frac{\omega}{c}$ . The region of these intercepts ( $\beta \leq \frac{\omega}{c}$ ) is not within the province of quasi-static analysis and their existence was correctly viewed with suspicion by Trivelpiece. His curves also indicate backward waves for small  $\beta b$ , a feature which is retained in the exact analysis only for small values of the parameter  $\frac{\omega_p b}{c}$ .

---

In the next section we consider the plasma column in large axial magnetic field. Modal properties in that case will be seen to differ significantly from those presented above for the opposite extreme of the unmagnetized column.

IV. THE PLASMA COLUMN IN LARGE AXIAL MAGNETIC FIELD

Large axial magnetic field is meant to imply an electron cyclotron frequency greatly in excess of either the electron plasma frequency or the signal frequency. This condition is not unrealistic for laboratory plasmas. Often a laboratory plasma has an axial magnetic field variable up to 20 kilogauss, which corresponds to a cyclotron frequency,  $f_c = 56 \text{ gc./sec.}$ , while a typical value of electron density might be  $10^{18} \text{ cm.}^{-3}$  which corresponds to a plasma frequency,  $f_p = 2.84 \text{ gc./sec.}$ ; it will be shown that for guided propagation the signal frequency is smaller than  $f_p$ . The large axial magnetic field will not interact with electron motion parallel to it but will effectively inhibit any transverse motion.

A. The Dispersion Curves

In the limit of large  $B_0$ , the capacitivy tensor of equation (2) becomes uniaxial

$$\underline{\underline{\epsilon}} \rightarrow \epsilon_0 \begin{bmatrix} 1 & 0 & 0 \\ 0 & 1 & 0 \\ 0 & 0 & 1 - \frac{\omega_p^2}{\omega^2} \end{bmatrix} \quad (49)$$

The wave equation (17) and (18) uncouple, and the equation in  $E_z$  transforms to Bessel's equation with eigennumber  $(1 - \frac{\omega_p^2}{\omega^2}) (\frac{\omega^2}{c^2} - \beta^2)$  while the equation in  $H_z$  becomes Bessel's equation with eigennumber  $(\frac{\omega^2}{c^2} - \beta^2)$ . Consequently,  $H_z$  is unaffected by the plasma and no guided TE modes are possible.

The axial component of  $\underline{E}$  will have the form

$$E_{z1} = F J_n\left(\frac{p_m r}{b}\right) e^{j(\omega t - \beta z - n\phi)} \quad (50)$$

$$p_m^2 = \left(\frac{\omega_p^2}{\omega^2} - 1\right) (\beta^2 b^2 - \frac{\omega^2}{c^2} b^2) = \left(\frac{\omega_p^2}{\omega^2} - 1\right) q^2 \quad (51)$$

For bound modes  $p_m$  is real imposing the constraint  $\omega < \omega_p$ .

The modes are TM having field components  $E_z$ ,  $E_r$ ,  $H_\phi$  for the  $n = 0$  case and all field components except  $H_z$  for  $n \geq 1$ . The characteristic equation may be found as outlined in the previous section and is

$$p_m \frac{J'_n(p_m)}{J_n(p_m)} = q \frac{K'_n(q)}{K_n(q)} \quad (52)$$

This equation has previously appeared in the literature.<sup>10</sup>

The left side of (52) is oscillatory and there will consequently be an infinity of solutions for a given  $n$ . The modes are then doubly infinite in number and a given mode will be designated by a double subscript as  $TM_{nm}$ .

The dispersion relationship is gotten by substituting in the characteristic equation for  $p_m$  and  $q$  in terms of  $\frac{\omega b}{c}$ ,  $\beta b$ , and  $\frac{\omega_p b}{c}$  as determined by equations (19) and (51). The dispersion relation is plotted for several modes in Fig. 8 with  $\frac{\omega_p b}{c} = 10$ .

The curves have similar shapes for different modes; they all begin at the origin and asymptotically approach the line  $\omega = \omega_p$  for large  $\beta$ . As in the zero field case the asymptotic approach is accompanied by resonant excitation of electron oscillations. Along the asymptote,  $q$  increases without bound, but the plasma eigennumber  $p_m$  remains



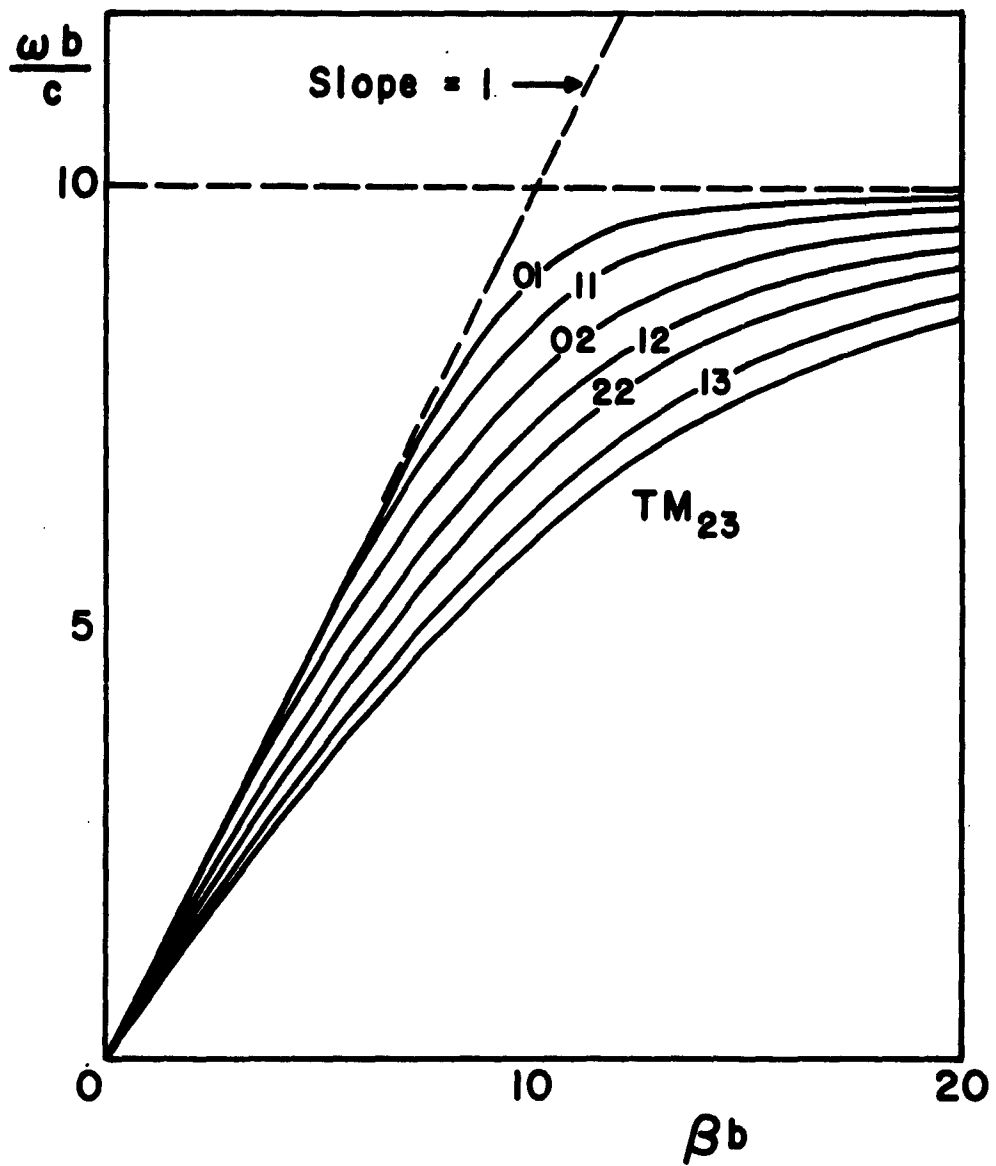


Figure 8 . Dispersion Curves for the Plasma Column  
with Large Axial Magnetic Field,  $\frac{\omega_p b}{c} = 10$

essentially constant, and the fields are concentrated in the body of the plasma rather than at the interface.

Fig. 8 also demonstrates that the waves become slower (i.e., phase and group velocity decrease) as the order of the mode increases. The initial slope of the dispersion curve may be shown to equal

$\left[ 1 + \left( \frac{\omega_p b}{c} \right)^{-2} z_{n-1,m}^2 \right]^{1/2}$  for the  $TM_{nm}$  mode, where  $z_{n-1,m}$  is the  $m$ th zero of  $J_{n-1}$  exclusive of the zero at the origin except for  $n = 0$ .

The initial slope of the  $TM_{01}$  mode is unity. Trivelpiece and Gould<sup>1</sup> found curves similar to Fig. 8 for a plasma filling a circular conducting pipe.

In that case the initial slopes of the curves were found to be

$\left[ 1 + \left( \frac{\omega_p b}{c} \right)^{-2} z_{nm}^2 \right]^{1/2}$  so that the waves are seen to be faster for the open column.

#### B. A Unique Waveguiding Feature

There is a rather unique feature of the equations for this case of large magnetic field which has interesting physical implications.

Equation (51) expresses  $p_m$  in terms of  $q$  independently of column radius,  $b$ , and the characteristic equation (52) also defines a relationship between the radial eigennumbers which is independent of  $b$ .

Thus either  $q$  or  $p_m$  may be determined as a function of the ratio  $\frac{\omega}{\omega_p}$  for arbitrary column radius.

Curves of  $q$  vs.  $\frac{\omega}{\omega_p}$  are plotted in Fig. 9 for several modes. That radial eigenvalues are independent of the transverse dimensions of the column may be associated with the fact that the portion of the capacitivity tensor pertaining to the coordinates transverse to the magnetic field is a scalar equal to  $\epsilon_0$ .

The effect on waveguiding properties of the column may be seen by considering equation (19) which we rewrite as

$$\beta^2 = \frac{\omega^2}{c^2} + \frac{q^2}{b^2} \quad (53)$$

For a fixed  $\omega_p$  and  $\omega$  (and therefore a fixed  $q$ ) as the column radius is increased phase velocity approaches the speed of light in vacuo (i.e.,  $\beta \rightarrow \frac{\omega}{c}$ ). Fig. 10 depicts the dependence of the dispersion curve for the  $TM_{01}$  mode on column radius  $b$ .

The tendency of the waves to become faster with increasing radius is opposite to the behaviour of an open dielectric rod waveguide. In the latter case, if the radius of the dielectric rod greatly exceed the wavelength in the dielectric, phase velocity is slowed to the speed of light in the dielectric,  $\frac{c}{\sqrt{\epsilon_r}}$ . On the other hand, if the radius of the plasma column is much larger than the wavelength, we approach the situation of having all the field energy stored in field components transverse to the direction of propagation (except at resonance) so that the effective capacitivity is  $\epsilon_0$  and phase velocity approaches  $c$ .

To calculate stored energy one uses the expression for average energy density appropriate to dispersive media

$$\bar{U} = \frac{1}{4} \text{Real} \left( \underline{H}^* \cdot \underline{B} + \underline{E}^* \cdot \frac{\partial(\omega \underline{\epsilon})}{\partial \omega} \cdot \underline{E} \right) \quad (54)$$

Then by substituting into (54) the appropriate field expressions for the mode under consideration which may be obtained from equations (50), (20), (15), and (16), and by integrating  $\bar{U}$  over the cross-section one may arrive at expressions for stored energy. Specifically, the ratio of energy in the transverse fields to that in the axial field for the  $TM_{01}$  mode is

$$\frac{\epsilon_z}{\epsilon_T} = \frac{b^2}{q^2} \left( 2 \frac{\omega^2}{c^2} + \frac{q^2}{b^2} \right) \frac{\left( \frac{\omega^2}{\omega_0^2} - 1 \right) K_0^2 (J_1^2 - J_0 J_2) - J_0^2 (K_1^2 - K_0 K_2)}{\left( \frac{\omega^2}{\omega_0^2} + 1 \right) K_0^2 (J_1^2 + J_0^2) + J_0^2 (K_1^2 - K_0^2)} \quad (55)$$

where the argument of the J's is  $p_m$

and the argument of the K's is  $q$

Equation (55) makes clear the increasing storage of energy in the transverse fields with increasing  $b$ .

As the signal frequency approaches the plasma frequency the augmented axial oscillations of the electrons near resonance is accompanied by increasing storage of energy in the axial field and the wave is slowed.

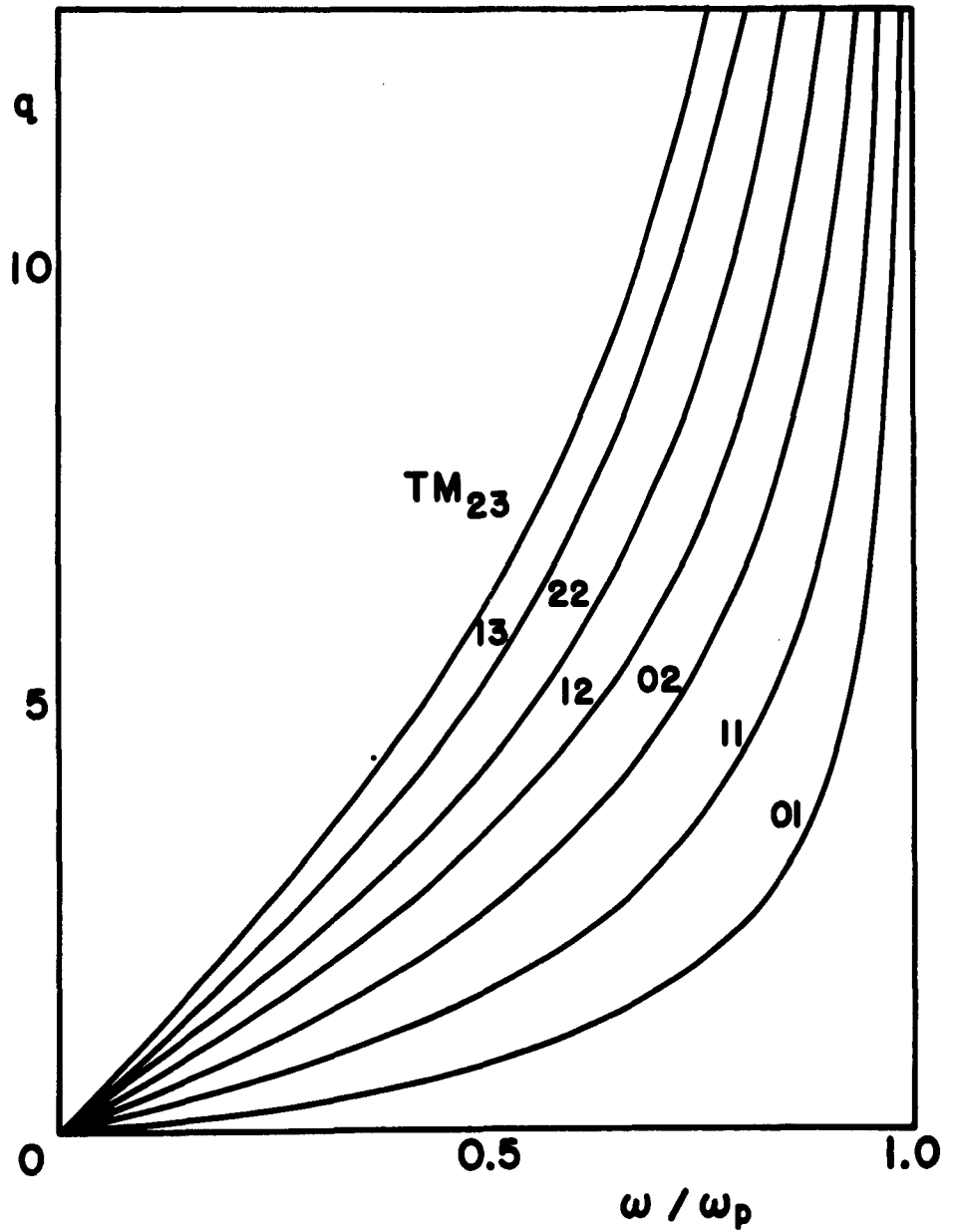


Figure 9 Index of Field Extent,  $q$ , as a Function of  $\omega/\omega_p$ .  
Plasma Column with Large Axial Magnetic Field

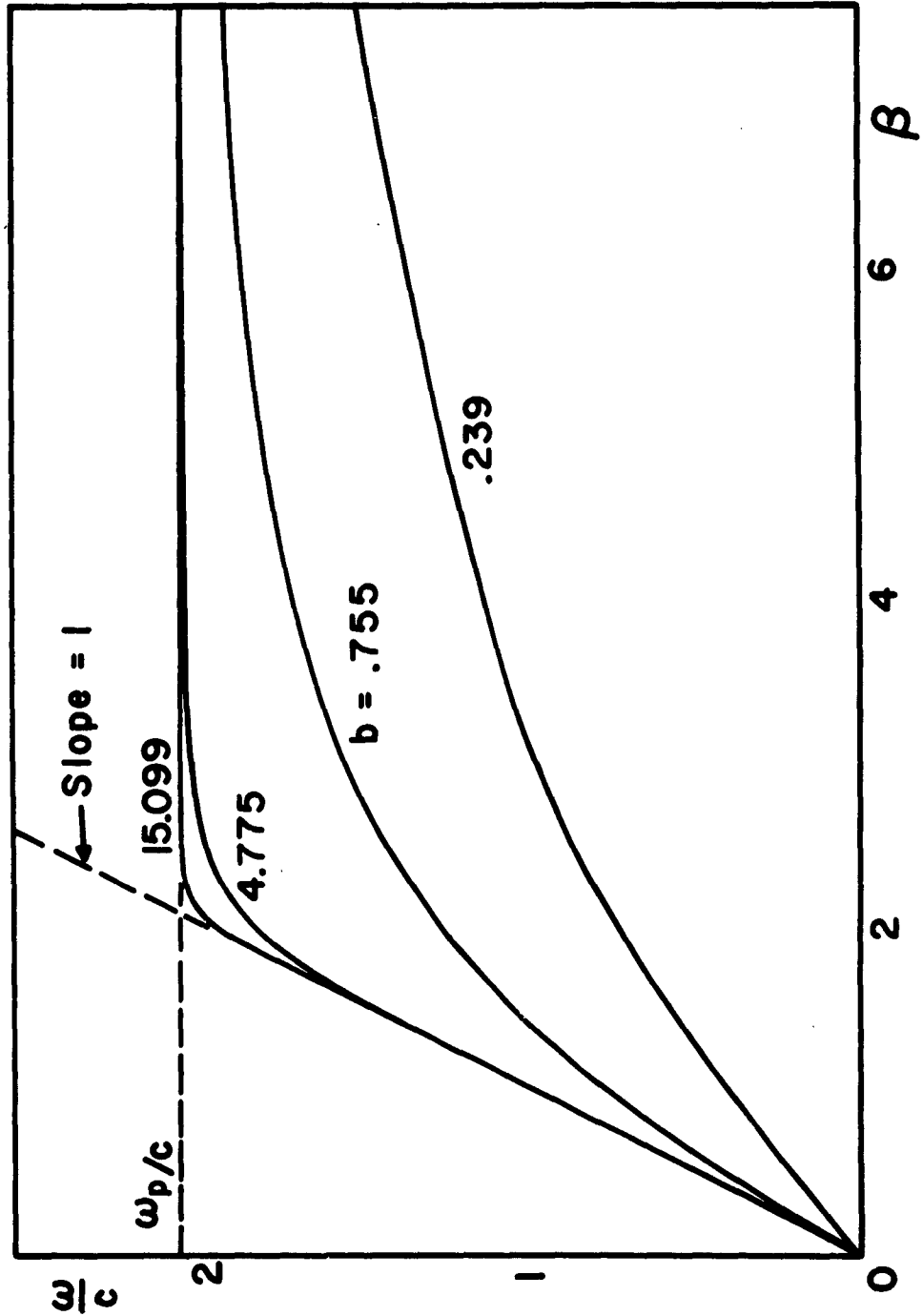


Figure 10 Dispersion Curves for the  $TM_{01}$  Mode with Column Radius,  $b$ , as Parameter.  $f_p = 10$  gc./sec. Plasma Column with Large Axial Magnetic Field.

## V. CONCLUSIONS

The properties of guided electromagnetic propagation along an unenclosed circular cylinder of plasma have been shown to contrast markedly for the two extremes of axial magnetic field.

For the case of zero magnetic field a single bound mode was found for each value of the integer  $n$  where the azimuthal variation of the modes is as  $e^{-jn\phi}$ . The azimuthally varying modes ( $n \geq 1$ ) are hybrid. The mode of one angular variation has no cutoff and its modal properties predicted by quasi-static analysis are significantly modified by the results of a more rigorous treatment. Modes of  $n > 1$  can exist only over a narrow range of frequency having a nonzero value of cutoff frequency. All modes experience a resonance at  $\omega = \frac{\omega_p}{\sqrt{2}}$  and are nonexistent at higher frequencies. The plasma fields vary radially as hyperbolic Bessel functions of the first kind,  $I_n$ . Perhaps the most significant feature is the appearance of backward waves for the azimuthally varying modes for small values of the parameter  $\frac{\omega_p b}{c}$ .

With large axial magnetic field there is an infinity of TM modes for each value of  $n$ . All modes begin at zero frequency and experience a resonance at  $\omega = \omega_p$  being nonexistent for  $\omega > \omega_p$ . The fields in the plasma region vary radially as Bessel functions of real argument,  $J_n$ . The radial eigennumbers are independent of column thickness, and phase velocity approaches the speed of light in vacuo if the column radius is large compared to the wavelength.

LIST OF REFERENCES

1. Trivelpiece, A.W., and Gould, R.W., "Space Charge Waves in Cylindrical Plasma Columns", J.A.P., Vol. 30, No. 11, pp. 1784-1793, November 1959.
2. Trivelpiece, A.W., "Slow Wave Propagation in Plasma Waveguides", Technical Report No. 7, California Institute of Technology, Pasadena, Calif., May 1958.
3. Linhart, J.G., "Plasma Physics", Interscience, New York, 1960, pp. 114-118.
4. Suhl and Walker, "Topics in Guided-Wave Propagation through Gyromagnetic Media", B.S.T.J., Vol. 33, pp. 579-659, pp. 939-986, pp. 1133-1194; 1954.
5. Bevc, V., and Everhart, T., "Fast Waves in Plasma-Filled Waveguides", A.S.D. Technical Report 61-14, Electronic Research Lab., University of California, Berkeley, Calif., July 1961.
6. Watson, G.N., "A Treatise on the Theory of Bessel Functions", Macmillan, New York, 1944.
7. Oliner, A.A., and Tamir, T., "Backward Waves on Isotropic Plasma Slabs", J.A.F., Vol. 33, No. 1, pp. 231-233, January 1962.
8. Landau, L., "On Vibrations of the Electronic Plasma", J. Phys. U.S.S.R., Vol. 10, No. 1, p. 25, 1946.
9. Stix, T.H., "Theory of Plasma Waves", McGraw-Hill, New York, 1962.
10. Dawson, J., and Oberman, C., "Oscillations of a Finite Cold Plasma in a Strong Magnetic Field", Physics of Fluids, Vol. 2, No. 2, pp. 103-111, March-April 1960.